

Nuclear-polarization contribution to the Lamb shift in actinide nuclei

Günter Plunien and Gerhard Soff

*Institut für Theoretische Physik, Technische Universität Dresden,
Mommssenstrasse 13, D-01062 Dresden, Federal Republic of Germany*

(Received 18 May 1994)

The contribution of nuclear polarization to the Lamb shifts of bound electrons in the $1s_{1/2}$, $2s_{1/2}$, and $2p_{1/2}$ states is considered for various even- A nuclei ($230 \leq A \leq 252$ with $90 \leq Z \leq 98$). Utilizing the concept of effective photon propagators with nuclear polarization insertions, the effective self-energy shifts due to virtual excitation of collective nuclear rotational and vibrational states and of the dominant giant dipole resonance are calculated. The formalism is extended to odd- Z nuclei for which the effective interaction is derived within the single-particle approach. While the corresponding energy shifts of the $1s_{1/2}$ state represent a considerable correction, the contribution to the $2s$ - $2p$ splitting is comparable to the current accuracy of high-precision experiments.

PACS number(s): 31.30.Jv, 12.20.Ds, 12.20.Fv, 32.90.+a

I. INTRODUCTION

Recent experimental abilities to prepare highly ionized atoms and even bare heavy nuclei up to the actinides allow for a new generation of high-precision experiments. One of the fascinating aspects is that studies with few-electron systems provide new sensitive tests of quantum electrodynamics in intense Coulomb fields. A direct measurement of the Lamb shift in lithiumlike uranium performed by Schweppe *et al.* [1] occurred to be more precise than theory at that time. Recent calculations performed by Blundell [2] are in fair agreement with experimental data within a tenth of an eV. In future experiments with hydrogenlike heavy atoms, the aimed precision in the determination of the ground state Lamb shift will be at the level of 0.1 eV. For comparison, the total $1s$ binding energy amounts to about 100 keV while the current theoretical uncertainty is estimated to be about 1 eV.

This excellent accuracy in measurements necessitates not only the inclusion of typical QED effects, such as self-energy, vacuum polarization, electron correlations, etc., even in higher order in α , together with finite-nuclear-size corrections [3–5]. It turns out that non-QED effects such as nuclear polarization can no longer be neglected [6, 7]. During the last decade the dominant QED corrections [2, 8–12] have been calculated. These intensive research activities are motivated by the fact that for atomic systems the underlying fundamental interaction is known. Thus, the comparison between theoretical results of *ab initio* calculations with corresponding experimental data allows for a direct test of our understanding of heavy few-electron systems. Therefore, any discrepancy between theory and experiment may either motivate an improvement of theoretical investigations and a refinement of experiments, or it may indicate the possible influence of non-QED effects. In this context, the study of nuclear polarization contributions to the total energy shift of atomic levels becomes important because, as a background effect, it represents a natural limitation of any high-precision test, which crucially depends on a precise knowledge of the spectrum of heavy electronic atoms.

In contrast to the QED-radiative corrections mentioned above, an *ab initio* evaluation of nuclear polarization is not practicable at the level of fundamental interactions. Accordingly, any calculation of nuclear polarization is inherently phenomenological and depends on the parameters of the nuclear model used to describe the intrinsic nuclear dynamics. During the past few decades, a lot of experience has been developed in calculating the nuclear-polarization effect for muonic atoms. There it leads to corrections at the keV level mainly because of the huge overlap of the muon-wave function with the nucleus and because the transition energies in muonic atoms are of the order of magnitude of typical nuclear excitation energies (e.g., see the review of Borie and Rinker [13] and references therein). Much less attention has been drawn to nuclear-polarization effects in electronic atoms. They turn out to be reduced by orders of magnitude, because of the small electron rest mass. The few calculations known to us were based on second-order Schrödinger perturbation theory [14, 15]. In an earlier paper [7] we have presented a relativistic, field-theoretical treatment of nuclear polarization utilizing the concept of effective photon interactions with nuclear-polarization insertions. This formalism allows a convenient and systematic treatment of nuclear polarization in terms of effective QED-radiative corrections with dressed internal photon lines. The more important fact is that, as a direct consequence of the relativistic approach, an additional vacuum contribution is derived, which is missing in earlier calculations. Although the formal setup is rather general, specific nuclear models have to be applied in order to determine the polarization function. Evidently, only virtual nuclear excitations with strong excitation strengths may contribute considerably to an energy correction. In fact, the energy shifts due to virtual collective nuclear excitations become important as indicated in Ref. [7].

In this paper, we shall perform a systematic study of the nuclear-polarization contribution due to collective nuclear excitations (vibrations, rotations, and giant dipole resonances) in even- A actinide nuclei in the region $Z \geq 90$ and $A \geq 230$. Numerical results for the

associated energy shift of $1s_{1/2}$, $2s_{1/2}$, and $2p_{1/2}$ states are presented for these nuclei. We shall also discuss how to include single-particle excitations of a valence proton in odd- A nuclei. A possible extension of the formalism based on a microscopic approach will be presented. Expressions for the transition density operator in terms of electric multipoles and the corresponding effective propagators will be derived. The single-particle basis used for deriving the effective propagator is specified within the Weisskopf approximation. The formal steps, which have to be performed in the case of a more general type of boson expansion approach, may already become transparent. Representing the polarization insertions in terms of boson expansions provides an alternative framework in order to treat collective nuclear excitations as well.

This paper is organized as follows. In Sec. II, we shall present a brief review of the basic formalism that allows for the treatment of nuclear polarization as effective radiative corrections. The different terms of the resulting formula for the energy shift will be discussed in some detail. Although the main purpose of this paper is to generate further numerical results for the contribution of nuclear polarization to the Lamb shift in even- A nuclei only, we shall present the formal extensions to odd- A nuclei, especially for those with one valence proton, in Sec. III. For collective nuclear models the expressions for the nuclear polarization insertions and the corresponding propagators will be summarized in the Appendix. In Secs. IV and V, numerical results for the contributions to the energy shift of electronic $1s_{1/2}$, $2s_{1/2}$, and $2p_{1/2}$ bound states will be presented.

II. FORMALISM

In a previous paper [7], we have demonstrated in detail that nuclear polarization can be treated within the framework of QED-perturbation theory as an effective radiative correction. The basic idea is to replace, in a given QED-Feynman diagram, the free photon propagator $D_{\mu\nu}(x-x')$ representing free internal photon lines by the modified part $\tilde{D}_{\mu\nu}(x, x')$ of the effective interaction $\mathcal{D}_{\mu\nu}(x, x')$, which accounts for the nuclear degrees of

freedom in terms of nuclear-polarization insertions. The Dyson equation for the effective photon propagator,

$$\begin{aligned} \mathcal{D}_{\mu\nu}(x, x') &= D_{\mu\nu}(x-x') + \tilde{D}_{\mu\nu}(x, x') \\ &= D_{\mu\nu}(x-x') + \int d^4x_1 d^4x_2 \\ &\quad \times D_{\mu\alpha}(x-x_1) \Pi^{\alpha\beta}(x_1, x_2) D_{\beta\nu}(x_2-x'), \end{aligned} \quad (1)$$

defines the modification $\tilde{D}_{\mu\nu}$ and, thus, the (reducible) nuclear-polarization tensor $\Pi^{\alpha\beta}$. The latter is given by the vacuum expectation value of the nuclear transition current density $\hat{j}_{\text{nuc}}^\alpha$ (Heisenberg operator):

$$i \Pi^{\alpha\beta}(x_1, x_2) = \langle \mathcal{O} | T \hat{j}_{\text{nuc}}^\alpha(x_1) \hat{j}_{\text{nuc}}^\beta(x_2) | \mathcal{O} \rangle. \quad (2)$$

The vacuum state $|\mathcal{O}\rangle$ implies that the nucleus is considered to be in its ground state. However, the exact transition current $\hat{j}_{\text{nuc}}^\alpha$ is not known from first principles. It can only be specified if particular nuclear models are applied. As a consequence, the effective interaction $\tilde{D}_{\mu\nu}$ becomes model dependent. A practicable evaluation requires further approximations. When calculating $\tilde{D}_{\mu\nu}$, we shall neglect possible distortions of the nuclear excitation spectrum due to the presence of the electron. These effects have to be taken into account in the case of muonic atoms. However, they are expected to be of minor importance in electronic atoms. Accordingly, the time evolution of the transition current $\hat{j}_{\text{nuc}}^\alpha$ is governed by the nuclear model Hamiltonian \hat{H}_{nuc} only, and $\Pi^{\alpha\beta}$ and $\tilde{D}_{\mu\nu}$ become homogeneous in time. For our purpose, we shall further neglect the contribution of the vector current $\hat{j}_{\text{nuc}}^\alpha$ because the velocities associated with the intrinsic nuclear dynamics are mainly nonrelativistic. Taking into account electric nuclear transitions only, we have to keep the component Π^{00} of the polarization tensor and we thus have to deal with the longitudinal part \tilde{D}_{00} of the effective propagator.

In lowest order perturbation theory in α (formulated in the Furry picture), the energy shift of an electron bound state ψ_i due to virtual nuclear excitations is given by a corresponding effective self-energy contribution and a vacuum-polarization term:

$$\begin{aligned} \Delta E_i^{\text{NP}} &= \Delta E_i^{\text{NP}}(\text{SE}) + \Delta E_i^{\text{NP}}(\text{VP}) \\ &= i\alpha \int d^3r_1 d^3r_2 \psi_i^\dagger(\vec{r}_1) \int dE S_F(\vec{r}_1, \vec{r}_2, E_i - E) \tilde{D}_{00}(\vec{r}_1, \vec{r}_2, E) \gamma^0 \psi_i(\vec{r}_2) \\ &\quad - i\alpha \int d^3r_1 d^3r_2 \psi_i^\dagger(\vec{r}_1) \psi_i(\vec{r}_1) \tilde{D}_{00}(\vec{r}_1, \vec{r}_2, E=0) \text{Tr}[\gamma^0 S_F(\vec{r}_2, \vec{r}_2, 0)]. \end{aligned} \quad (3)$$

The Fourier-transformed electron propagator S_F satisfies the equation

$$\begin{aligned} \{E - [i\gamma^0 \vec{\gamma} \cdot \vec{\nabla} + eA_{\text{ext}}^0(\vec{r}) + \gamma^0 m]\} S_F(\vec{r}, \vec{r}', E) \\ = \gamma^0 \delta^3(\vec{r} - \vec{r}'). \end{aligned} \quad (4)$$

The bound state ψ_i is a solution of the Dirac equation in

the static external Coulomb field A_{ext}^0 of an extended nucleus, which is described by a static, classical charge density distribution ρ_{ext} characterizing the ground state. In contrast to the situation in muonic atoms the particular details of the ground-state charge density are again of minor importance here. We should also note, that the effect of static nuclear deformation on the energy of electronic levels can be treated separately by means of ordinary

perturbation theory. In our calculations of nuclear polarization, a homogeneously charged sphere is used to describe the nuclear ground-state charge distribution. Accordingly, the contribution of the vacuum-polarization part [second term of Eq. (3)] becomes negligible. The spherically symmetric external Coulomb field A_{ext}^0 induces a (renormalized) vacuum-polarization charge density $\rho_{\text{vac}}(\vec{r}) = i \{ \text{Tr}[\gamma^0 S_F(\vec{r}, \vec{r}, 0)] \}_{\text{ren}}$, which is spherical too. It is easily verified by means of the angular momentum decomposition of the effective propagator \tilde{D}_{00} , that a spherically symmetric vacuum-polarization charge density can only couple to nuclear monopole excitations. In the case of collective nuclear excitations with multipolarity $L > 0$, this term in fact does not contribute to the energy shift ΔE_i^{NP} . Thus, we are left with the nuclear-polarization contribution, which corresponds to the effective self-energy [first term of Eq. (3)].

The derivation of the effective interaction \tilde{D}_{00} is performed in the Coulomb gauge:

$$\tilde{D}_{00}(\vec{r}, \vec{r}', E) = \int d^3r_1 d^3r_2 \frac{1}{|\vec{r} - \vec{r}_1|} \Pi^{00}(\vec{r}_1, \vec{r}_2, E) \frac{1}{|\vec{r}_2 - \vec{r}'|}. \quad (5)$$

What is left so far is to specify the polarization function Π^{00} . It can be formally represented as

$$\begin{aligned} \Pi^{00}(\vec{r}, \vec{r}', E) &= \sum_{\nu} \left\{ \left\langle \mathcal{O} \left| \frac{\hat{\rho}_{\text{nuc}}(\vec{r}, 0)}{E - \hat{H}_{\text{nuc}} + i\eta} \right| \nu \right\rangle \langle \nu | \hat{\rho}_{\text{nuc}}(\vec{r}', 0) | \mathcal{O} \rangle \right. \\ &\quad \left. - \left\langle \mathcal{O} \left| \frac{\hat{\rho}_{\text{nuc}}(\vec{r}', 0)}{E + \hat{H}_{\text{nuc}} - i\eta} \right| \nu \right\rangle \langle \nu | \hat{\rho}_{\text{nuc}}(\vec{r}, 0) | \mathcal{O} \right\}, \end{aligned} \quad (6)$$

$$\begin{aligned} \tilde{D}_{00}(\vec{r}, \vec{r}', E) &= \sum_{\nu} \sum_{LMi L'M'i'} \left\{ \frac{\langle \mathcal{O} | \hat{Q}_{LM}^{(i)} | \nu \rangle \langle \nu | \hat{Q}_{L'M'}^{(i)\dagger} | \mathcal{O} \rangle}{E - E_{\nu} + i\eta} - \frac{\langle \mathcal{O} | \hat{Q}_{L'M'}^{(i)\dagger} | \nu \rangle \langle \nu | \hat{Q}_{LM}^{(i)} | \mathcal{O} \rangle}{E + E_{\nu} - i\eta} \right\} \\ &\quad \times F_L^{(i)}(r) F_{L'}^{(i)}(r') Y_{LM}(\hat{r}) Y_{L'M'}^*(\hat{r}'), \end{aligned} \quad (9)$$

where E_{ν} denotes the excitation energy of the nuclear state $|\nu\rangle$. The radial functions $F_L^{(i)}$ are given by

$$\begin{aligned} F_L^{(i)}(r) &= \frac{4\pi}{2L+1} \left[\frac{1}{r^{L+1}} \int_0^r dr_1 r_1^{L+2} \mathcal{R}_L^i(r_1) \right. \\ &\quad \left. + r^L \int_r^{\infty} dr_1 r_1^{-L+1} \mathcal{R}_L^i(r_1) \right]. \end{aligned} \quad (10)$$

At this point one has to specify the nuclear excitation modes $|\nu\rangle$ to be taken into account. Any particular nucleus under consideration requires an adequate choice for the nuclear model to describe relevant excitations. It can be shown that Eq. (9) for the modified propagator is valid under rather general conditions. A decomposition of the charge density fluctuation according to (7) is valid not only in the case of collective nuclear excitations (surface vibrations, rotations, and giant resonances) treated within collective nuclear models [17]. A similar

where a complete set of excited nuclear states $|\nu\rangle$ has been inserted. Normal ordering is indicated by $::$. For later purposes, we shall assume that the states $|\nu\rangle$ are eigenstates of the nuclear model Hamiltonian describing the intrinsic nuclear dynamics. Under rather general conditions, we can decompose the transition charge density $\hat{\rho}_{\text{nuc}}(\vec{r})$ (one-particle operator) in terms of electric multipoles $\hat{Q}_{LM}^{(i)}$ referring to nuclear transitions, which are characterized by angular momentum L and projection M (and perhaps additional relevant quantum numbers abbreviated by i):

$$\hat{\rho}_{\text{nuc}}(\vec{r}) = \sum_{LMi} \mathcal{R}_L^i(r) Y_{LM}(\hat{r}) \hat{Q}_{LM}^{(i)}. \quad (7)$$

Since $\hat{\rho}_{\text{nuc}}$ transforms as a scalar under spatial rotations, the operators $\hat{Q}_{LM}^{(i)}$ transform as spherical tensors of rank L with the property $\hat{Q}_{LM}^{(i)\dagger} = (-)^L \hat{Q}_{L-M}^{(i)}$. They are related to the total electric multipole operator \hat{Q}_{LM} via

$$\hat{Q}_{LM} = \int d^3r r^L Y_{LM}^*(\hat{r}) \hat{\rho}_{\text{nuc}}(\vec{r}) = \sum_i C_L^i \hat{Q}_{LM}^{(i)}, \quad (8)$$

where the radial parts $\mathcal{R}_L^i(r)$ of the transition density are strongly localized functions, such that the real constants $C_L^i = \int_0^{\infty} dr r^{L+2} \mathcal{R}_L^i(r)$ remain finite. Insertion of the expansion (7) into Eq. (6) and performing integrations according to the definition (5), we obtain for the modified propagator,

representation is also obtained within a microscopic approach provided the Weisskopf approximation for the nuclear single-particle states is applied. The latter implies to represent operators and single-particle states within the spherical basis and assuming that the radial part of the wave functions are constant inside the nucleus. Under these conditions, an equivalent consistent multipole decomposition of the charge density fluctuation (7) can be easily derived. We refer to Sec. III, where explicit expressions for the electric multipole operator \hat{Q}_{LM} and the radial functions \mathcal{R}_L are derived. Consequently, the complete set of eigenstates $|\nu\rangle$ of the nuclear Hamiltonian \hat{H}_{nuc} should be specified in the spherical representation as well, in order to achieve a direct evaluation of the matrix elements involved in the expressions for Π^{00} , respectively, \tilde{D}_{00} .

When evaluating \tilde{D}_{00} in the single-particle approach, we have to distinguish between even A (even Z) and between odd- A (odd- Z) nuclei. In the case of even- A nuclei

the ground state $|\mathcal{O}\rangle$ has zero total angular momentum, i.e., $J_{\mathcal{O}} = 0$. The excited states $|\nu\rangle \equiv |J_{\nu}M_{\nu}\rangle$ are in principle arbitrary linear combinations of one-particle-one-hole states (neglecting higher particle-hole correlation terms for simplicity) coupled to total angular momentum J_{ν} forming the collective states. In the case of odd- A nuclei the ground state $|\mathcal{O}\rangle$ has a finite angular momentum equal to that of the valence proton. For reasons of simplicity, let us consider nuclei with a ground state of the form $|\mathcal{O}\rangle \equiv |v\rangle := |J_v M_v\rangle = \hat{a}_{J_v M_v}^{\dagger} |\widetilde{\mathcal{O}}\rangle$. Here, $|\widetilde{\mathcal{O}}\rangle$ denotes the vacuum of the even- A core and $\hat{a}_{J_v M_v}^{\dagger}$ denotes the creation operator for the valence proton in its ground state characterized by an angular momentum J_v . It should be mentioned that the evaluation of matrix elements involving this odd- A vacuum state implies a summation over all projections M_v due to possible degeneracies of the ground state. Two types of nuclear excitations now contribute to the summation over intermediate states in Eq. (9). First, the valence nucleon can undergo transitions into an excited state $|\nu'\rangle$, while the core remains in its ground state $|\widetilde{\mathcal{O}}\rangle$. Second, the core can be excited, similar as the neighboring even- $(Z-1)$ nucleus, while the valence proton remains unaffected. Collective core excitations now give rise to characteristic multiplets in the excitation spectrum according to the coupling of the angular momentum referring to the core excitation and that of the valence nucleon. The polarization function and, thus, the effective propagator decomposes into a collective part describing collective nuclear excitations of the core and a single-particle contribution due to excitations of the valence nucleon. Thus, the modified propagator can be written in the form

$$\begin{aligned} \tilde{D}_{00}(\vec{r}, \vec{r}', E) &= \sum_{LM} \left[\sum_{\text{coll}} B^{\text{coll}}(EL; L \rightarrow 0) \right. \\ &\quad \times \frac{2EL}{E^2 - E_L^2 + i\eta} F_L^{\text{coll}}(r) F_L^{\text{coll}}(r') \\ &\quad + B^{\text{SP}}(EL; J_v \rightarrow J_{v'}) \frac{2EJ_{v'}}{E^2 - E_{J_{v'}}^2 + i\eta} \\ &\quad \left. \times F_L^{\text{SP}}(r) F_L^{\text{SP}}(r') \right] Y_{LM}(\hat{r}) Y_{LM}^*(\hat{r}'), \\ B^{\text{coll}}(EL; L \rightarrow 0) &= \frac{B^{\text{coll}}(EL; 0 \rightarrow L)}{2L + 1} \\ &= \frac{|\langle \mathcal{O} | \hat{Q}_L | L \rangle|^2}{2L + 1}, \\ B^{\text{SP}}(EL; J_v \rightarrow J_{v'}) &= \frac{|\langle J_v | \hat{Q}_L | J_{v'} \rangle|^2}{2J_v + 1}, \end{aligned} \quad (11)$$

where $J_{v'} = J_v + L$. While the first term represents the contributions due to various collective nuclear excitations, the second term only contributes in the case of odd- A nuclei. For a derivation of Eq. (11), we refer to the next section and to the Appendix, where expressions for the functions $F_L^{\text{SP}}(r)$, respectively, $F_L^{\text{coll}}(r)$ can be found. The effective propagator exclusively depends on phenomenological quantities like transition energies E_L and corresponding electric transition strengths [$B(EL)$ values]. The radial dependence carried by the functions

$F_L^{(i)}$ is determined by the one of the transition charge density \mathcal{R}_L^i (here the label i distinguishes between collective and single-particle excitations, respectively). As we have mentioned above, the details of the r dependence of the ground-state charge distribution ρ_{ext} is of minor importance for the energy shift in electronic atoms. Similar arguments hold concerning the r dependence of \mathcal{R}_L and, thus, for the functions F_L . The common feature of these functions is that they are strongly localized inside or near the surface of the nucleus. In the study of even- A nuclei, we are mainly interested in the contribution to the Lamb shift due to virtual excitations of collective surface vibrations, low-lying rotational modes, and the giant (dipole) resonance. In the case of even- A nuclei, collective nuclear excitations are of major importance. These modes can be treated employing the concepts of boson expansions (see, e.g., [16]) or geometrically motivated collective models [17]. Following the geometrical and hydrodynamic description [17] expressions for $B(EL)$ values and F_L can be derived (see Appendix). In our calculations we shall use experimental values for the transition strengths and excitation energies, if available. Let us only mention that an application of Eq. (11) including single-particle excitations would be the relevant calculation of the nuclear-polarization effect for ^{209}Bi .

Having derived the expression for \tilde{D}_{00} , we are now in the position to evaluate the effective self-energy contribution. Inserting the representation (11) together with the eigenfunction expansion for the Dirac propagator S_F ,

$$S_F(\vec{r}, \vec{r}', E) = \sum_k \frac{\psi_k(\vec{r}) \bar{\psi}_k(\vec{r}')}{E - E_k + \text{sgn}(E_k - E_F) i\eta}, \quad E_F = -1, \quad (12)$$

and using the spherical representation of the Dirac states (ν_1 denotes the principle quantum number of bound states, respectively, the energy of a continuum state)

$$\psi_k(\vec{r}) \equiv \psi_{\nu_1 \kappa_1 \mu_1}(\vec{r}) = \frac{1}{r} \begin{pmatrix} g_{\nu_1 \kappa_1}(\hat{r}) \chi_{\kappa_1 \mu_1}(\hat{r}) \\ i f_{\nu_1 \kappa_1}(\hat{r}) \chi_{-\kappa_1 \mu_1}(\hat{r}) \end{pmatrix}, \quad (13)$$

the following expression for the effective self-energy shift of a given bound state $\psi_{\nu\kappa\mu}$ characterized by a principal quantum number ν and angular momentum quantum numbers κ and μ due to collective nuclear excitations is obtained after some algebra:

$$\begin{aligned} \Delta E_{\nu\kappa\mu} &= -\alpha \sum_{L\kappa_1} B(EL; L \rightarrow 0) |\kappa_1| \\ &\quad \times \left(j_1 j L \left| \frac{1}{2} - \frac{1}{2} 0 \right. \right) \mathcal{M}_{\nu\kappa|\kappa_1}^L, \\ \mathcal{M}_{\nu\kappa|\kappa_1}^L &= \int_1^{\infty} dE' \frac{|\langle \nu\kappa | F_L | E' \kappa_1 \rangle|^2}{E' - E_{\nu\kappa} + E_L} \\ &\quad + \sum_{\nu_1} \frac{|\langle \nu\kappa | F_L | \nu_1 \kappa_1 \rangle|^2}{E_{\nu_1 \kappa_1} - E_{\nu\kappa} + E_L + i\eta} \\ &\quad + \int_{-\infty}^{-1} dE' \frac{|\langle \nu\kappa | F_L | E' \kappa_1 \rangle|^2}{E' - E_{\nu\kappa} - E_L}. \end{aligned} \quad (14)$$

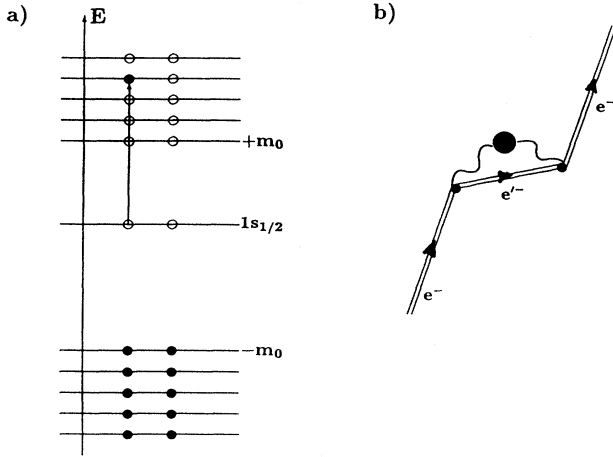


FIG. 1. The $1s_{1/2}$ electron can be virtually excited into an unoccupied state of the positive energy continuum via the interaction with virtual nuclear excitations (a). The corresponding Feynman diagram (b) represents the first two terms contributing to $\Delta E_{1s_{1/2}}$ [Eq. (14)].

First, we note that this contribution of nuclear polarization to the total Lamb shift carries an overall minus sign, i.e., $\Delta E_{\nu\kappa\mu}$ is negative and thus tends to increase the binding energy of electronic bound states. The effective self-energy shift depends parametrically on the excitation energies E_L , the corresponding $B(EL)$ values and, in principle, on the particular radial dependence F_L referring to the collective nuclear multipole transitions under consideration. The first two terms in $\mathcal{M}_{\nu\kappa|\kappa_1}^L$ describe transitions of the electron in the state $|\nu\kappa\mu\rangle$ into

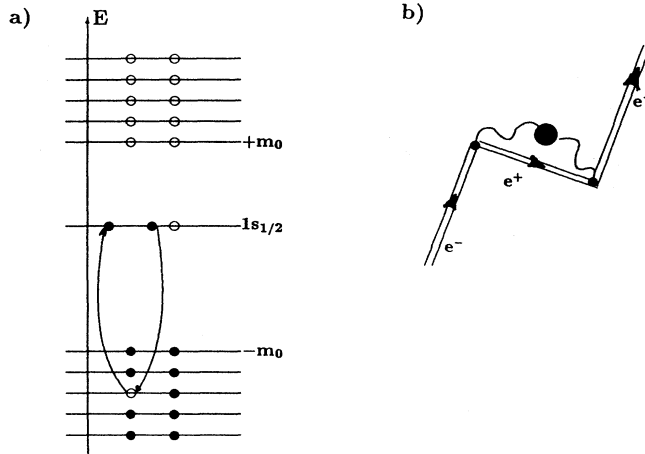


FIG. 2. An electron from the occupied negative energy continuum can be virtually excited into the occupied $1s_{1/2}$ state at different space-time points via the interaction with virtual nuclear excitations. The created positron annihilates with the $1s$ electron, which already had been present (a). The corresponding Feynman diagram of this “exchange” process (b) represents the vacuum contribution [third term of Eq. (14)] to $\Delta E_{1s_{1/2}}$.

higher unoccupied electron states due to virtual nuclear excitation. This intermediate state is either a positive energy continuum state $|E'\kappa_1\rangle$ (first term) or a bound state $|\nu_1\kappa_1\rangle$ (second term). These two terms are equivalent to the usual expressions derived in second-order perturbation theory. However, the third term in $\mathcal{M}_{\nu\kappa|\kappa_1}^L$ is a pure vacuum effect as a consequence of the relativistic, field-theoretical treatment, which accounts for the different time orderings. It describes the interaction of the Dirac vacuum with virtual nuclear excitations where an electron from the (occupied) Dirac sea $|E'\kappa_1\rangle$ can be excited into the occupied bound state $|\nu\kappa\mu\rangle$ at different space-time points, while the present electron and the positron (hole) will annihilate. This “exchange” process has first been taken into account in Ref. [7]. It should be mentioned, that this vacuum contribution is not included in earlier calculations of the effect of nuclear polarization in muonic atoms. The various processes contributing to $\Delta E_{\nu\kappa\mu}$ are illustrated in Figs. 1 and 2 for the $1s_{1/2}$ state.

III. MICROSCOPIC APPROACH TO NUCLEAR POLARIZATION

A microscopic description of the nuclear polarization starts with the representation of the charge density fluctuation operator (one-particle operator),

$$\hat{\rho}_{\text{fluc}}(\vec{r}) = e \sum_{i \neq j} \hat{a}_i^\dagger \hat{a}_j \phi_i^*(\vec{r}) \phi_j(\vec{r}), \quad (15)$$

where \hat{a}_i^\dagger (\hat{a}_i) denotes the creation (annihilation) operator of a nucleon, i.e., a proton, in the single-particle state ϕ_i . The electric multipole transition operator is obtained via

$$\hat{Q}_{LM} = \sum_{i \neq j} \hat{a}_i^\dagger \hat{a}_j Q_{LM}^{i,j}, \quad (16)$$

$$Q_{LM}^{i,j} = e \int d^3r \phi_i^*(\vec{r}) r^L Y_{LM}(\hat{r}) \phi_j(\vec{r}).$$

Particle and hole creation (annihilation) operators are introduced with respect to an appropriately chosen vacuum $|\mathcal{O}\rangle$, where all single-particle states are occupied up to the Fermi level F . In the case of an even- A nucleus $|\mathcal{O}\rangle$ is identical with its physical ground state, i.e., $|\mathcal{O}\rangle \equiv |\mathcal{G}\rangle$, while it is chosen as the ground state of an even- A core, in the case of an odd- A nucleus. We define the vacuum $|\mathcal{O}\rangle$ and particle (\hat{a}_p^\dagger) and hole (\hat{b}_q^\dagger) creation operators:

$$|\mathcal{O}\rangle = \prod_k^F \hat{a}_k^\dagger |0\rangle, \quad \hat{a}_p^\dagger = \hat{a}_{i>F}^\dagger, \quad \hat{a}_p |\mathcal{O}\rangle = 0, \quad \hat{b}_q^\dagger = \hat{a}_{i<F}^\dagger, \quad \hat{b}_q |\mathcal{O}\rangle = 0, \quad (17)$$

and the corresponding nuclear ground state for

$$|\mathcal{O}\rangle := |\mathcal{G}\rangle, \quad \text{even-}A \quad (18)$$

$$|\mathcal{O}\rangle \equiv |v\rangle := \hat{a}_v^\dagger |\mathcal{G}\rangle, \quad \text{odd-}A$$

where, for reasons of simplicity only, one valence nucleon

(proton) is assumed. The definitions (15)–(18) allow us to indicate the spectral representation of the polarization function Π^{00} . All operators can be alternatively expressed in terms of particle and hole operators (17).

We now introduce the spherical basis, i.e., relevant quantum numbers are specified as $i \rightarrow (J_i M_i)$, together with the states $\phi_i \rightarrow \phi_{J_i M_i}$ (shell model basis). Furthermore, we apply the Weisskopf approximation:

$$\phi_{J_i M_i}(\vec{r}) = f_{J_i}(r) Y_{J_i M_i}(\hat{r}), \quad (19)$$

where the radial functions are assumed to be constant inside the nucleus, such that for the matrix elements,

$$\langle f_{J_i} | r^L | f_{J_j} \rangle = \int_0^\infty dr' r'^{2+L} f_{J_i}(r') f_{J_j}(r') = \left(\frac{3R_0^L}{3+L} \right) \quad (20)$$

holds. This equation implies normalized radial functions,

$$f_{J_i}(r) = \left(\frac{3}{R_0^3} \right)^{\frac{1}{2}} \Theta(R_0 - r), \quad (21)$$

which are also independent of J_i . Under the assumptions (19)–(21) a consistent decomposition of $\hat{\rho}_{\text{nuc}}$ into multipoles \hat{Q}_{LM} of the form (7) can be derived. Only the radial functions \mathcal{R}_L need to be determined. Evaluation of \hat{Q}_{LM} according to Eq. (16) with the states (19) and insertion into (7) leads to

$$\begin{aligned} \hat{\rho}_{\text{nuc}}(\vec{r}) &= e \sum_{LM} \mathcal{R}_L(r) Y_{LM}(\hat{r}) \\ &\times \sum_{i \neq j} \hat{a}_{J_i M_i}^\dagger \hat{a}_{J_j M_j} \langle f_{J_i} | r^L | f_{J_j} \rangle \\ &\times \int d\hat{r}' Y_{J_i M_i}^*(\hat{r}') Y_{LM}^*(\hat{r}') Y_{J_j M_j}(\hat{r}'), \quad (22) \end{aligned}$$

where the summations over i and j imply summations over corresponding angular momenta and projections. Requiring that the product $\mathcal{R}_L(r) \langle f_{J_i} | r^L | f_{J_j} \rangle \equiv \mathcal{R}(r)$ is independent of L , the summations over L and M can be performed first:

$$\hat{\rho}_{\text{nuc}}(\vec{r}) = e \sum_{i \neq j} \hat{a}_{J_i M_i}^\dagger \hat{a}_{J_j M_j} \mathcal{R}(r) Y_{J_i M_i}^*(\hat{r}) Y_{J_j M_j}(\hat{r}). \quad (23)$$

If we identify the radial function \mathcal{R} with the radial parts of the nuclear transition densities obtained in the Weisskopf approximation, i.e., $\mathcal{R}(r) = f_{J_i}(r) f_{J_j}(r)$, the following consistent and equivalent representation of the charge density fluctuation operator can be derived:

$$\begin{aligned} \hat{\rho}_{\text{nuc}}(\vec{r}) &= \sum_{LM} \left(\frac{3+L}{R_0^{L+3}} \right) \Theta(R_0 - r) Y_{LM}(\hat{r}) \hat{Q}_{LM}, \\ \hat{Q}_{LM} &= e \left(\frac{3R_0^L}{3+L} \right) \sum_{i \neq j} \hat{a}_{J_i M_i}^\dagger \hat{a}_{J_j M_j} C_{LM}^{J_i M_i, J_j M_j}, \\ C_{LM}^{J_i M_i, J_j M_j} &= \sqrt{\frac{(2J_i+1)(2J_j+1)}{4\pi(2L+1)}} (J_i J_j L | 000) (-)^{M_i} \\ &\times (J_i J_j L | -M_i M_j M). \quad (24) \end{aligned}$$

The electric multipole transition operator may be expressed in terms of particle-hole operators:

$$\begin{aligned} \hat{Q}_{LM} &= e \left(\frac{3R_0^L}{3+L} \right) \left\{ \sum_{p \neq p'} \hat{a}_{J_p M_p}^\dagger \hat{a}_{J_{p'} M_{p'}} C_{LM}^{J_p M_p, J_{p'} M_{p'}} \right. \\ &- \sum_{q \neq q'} \hat{b}_{J_q M_q}^\dagger \hat{b}_{J_q M_q} C_{LM}^{J_q M_q, J_q M_q} \\ &+ \sum_{pq} \hat{b}_{J_q M_q} \hat{a}_{J_p M_p} C_{LM}^{J_q M_q, J_p M_p} \\ &\left. + \sum_{pq} \hat{a}_{J_p M_p}^\dagger \hat{b}_{J_q M_q} C_{LM}^{J_p M_p, J_q M_q} \right\}. \quad (25) \end{aligned}$$

In the following, we shall specify the excited nuclear states $|\nu\rangle$ in the shell model basis and derive expressions for the effective propagator \tilde{D}_{00} for even- A and odd- A nuclei.

In the case of even- A nuclei collective excitations $|L_\nu M_\nu\rangle$ may be described predominantly as linear combination of $1p$ - $1h$ states:

$$\begin{aligned} |L_\nu M_\nu\rangle &= \sum_{J_p J_q} C_{J_p J_q}^{L_\nu} \sum_{M_p M_q} (-)^{M_p} \\ &\times (J_p J_q L_\nu | -M_p M_q M_\nu) \hat{a}_{J_p M_p}^\dagger \hat{b}_{J_q M_q}^\dagger |\widehat{\mathcal{O}}\rangle, \\ : \hat{H}_{\text{nuc}} : |L_\nu M_\nu\rangle &= E_{L_\nu} |L_\nu M_\nu\rangle. \quad (26) \end{aligned}$$

The states $|L_\nu M_\nu\rangle$ are assumed to be eigenstates of a corresponding nuclear (model) Hamiltonian \hat{H}_{nuc} . Due to the algebraic structure of these states, the matrix elements of the electric transition operator, which occur in the expression for Π^{00} and \tilde{D}_{00} turn out to be related to the reduced transition strengths [18]:

$$\begin{aligned} &\sum_{M_\nu} \langle \mathcal{O} | \hat{Q}_{LM} | L_\nu M_\nu \rangle \langle L_\nu M_\nu | \hat{Q}_{L'M'}^\dagger | \mathcal{O} \rangle \\ &= \delta_{LL'} \delta_{L'L_\nu} \delta_{MM'} \frac{|\langle \mathcal{O} | \hat{Q}_{L_\nu} | L_\nu \rangle|^2}{2L_\nu + 1} \\ &= \delta_{LL'} \delta_{L'L_\nu} \delta_{MM'} B^{\text{coll}}(EL_\nu; L_\nu \rightarrow 0). \quad (27) \end{aligned}$$

The effective propagator \tilde{D}_{00} is obtained according to Eq. (9):

$$\begin{aligned} \tilde{D}_{00}(\vec{r}, \vec{r}', E) &= \sum_{LM} B^{\text{coll}}(EL; L \rightarrow 0) \frac{2E_L}{E^2 - E_L^2 + i\eta} \\ &\times F_L^{\text{SP}}(\tau) F_L^{\text{SP}}(\tau') Y_{LM}(\hat{r}) Y_{LM}^*(\hat{r}'), \quad (28) \end{aligned}$$

where F_L^{SP} has to be evaluated according to Eq. (10) with the radial function $\mathcal{R}_L = \frac{3+L}{R_0^{L+3}} \Theta(R_0 - r)$:

$$\begin{aligned}
F_L^{\text{SP}}(r) &= \frac{4\pi}{(2L+1)R_0^L} \tilde{F}_L^{\text{SP}}(r), \\
\tilde{F}_L^{\text{SP}}(r) &= \Theta(R_0 - r) \left[\frac{r^2}{R_0^3} \right. \\
&\quad \left. + \begin{cases} -\frac{5r^2}{R_0^3} \ln(r/R_0) & \text{for } L = 2 \\ \left(\frac{3+L}{L-2} \right) \left(\frac{r^2}{R_0^3} - \frac{r^L}{R_0^{L+1}} \right) & \text{for } L \neq 2 \end{cases} \right] \\
&\quad + \Theta(r - R_0) \frac{R_0^L}{r^{L+1}}. \quad (29)
\end{aligned}$$

The resulting propagator (28) has exactly the same structure as those derived for collective vibrations, rotations, and giant resonances [7]. Slight modifications occur in the radial dependence (29) inside of the nucleus, which is the only residue of the single-particle interpretation.

In the case of odd- A nuclei, i.e., an even- A core plus one valence proton, two types of nuclear excitations contribute to the effective propagator. The first type are single-particle excitations of the valence proton (indicated by primes):

$$\begin{aligned}
|J_{v'} M_{v'}\rangle &= \hat{a}_{J_{v'}, M_{v'}}^\dagger |\widetilde{\mathcal{O}}\rangle, \\
:\hat{H}_{\text{nuc}}: |J_{v'} M_{v'}\rangle &= E_{J_{v'}} |J_{v'} M_{v'}\rangle, \quad (30)
\end{aligned}$$

where the core remains in its ground state $|\widetilde{\mathcal{O}}\rangle$. The second type are collective excitations of the $(Z-1)$ core giving rise to a multiplet of single-particle states,

$$\begin{aligned}
|J_\nu M_\nu\rangle &= \sum_{M_\nu m} (J_\nu l J_\nu | M_\nu m M_\nu) \hat{a}_{J_\nu, M_\nu}^\dagger |lm\rangle, \\
:\hat{H}_{\text{nuc}}: |J_\nu M_\nu\rangle &= E_{J_\nu, M_\nu} |J_\nu M_\nu\rangle, \\
J_\nu &= |J_\nu - l|, \dots, J_\nu + l, \quad (31)
\end{aligned}$$

where the states $|lm\rangle$ are again linear combinations as

indicated in Eq. (26). A multiplet of states arising from collective core excitations consists of $2l+1$ states $|J_\nu M_\nu\rangle$, which are concentrated close to an average energy \bar{E}_l that would correspond to a collective excitation of the neighboring even- $(Z-1)$ nucleus.

Having specified the nuclear states, in a next step the matrix elements with the transition operator have to be calculated. Excitations of the valence proton lead to

$$\begin{aligned}
&\sum_{M_{v'}} \langle \mathcal{O} | \hat{Q}_{LM} | J_{v'} M_{v'} \rangle \langle J_{v'} M_{v'} | \hat{Q}_{L'M'}^\dagger | \mathcal{O} \rangle \\
&= \sum_{M_v M_{v'}} \langle J_v M_v | \hat{Q}_{LM} | J_{v'} M_{v'} \rangle \langle J_{v'} M_{v'} | \hat{Q}_{L'M'}^\dagger | J_v M_v \rangle \\
&= \delta_{LL'} \delta_{MM'} B^{\text{SP}}(EL; J_v \rightarrow J_{v'}), \quad (32)
\end{aligned}$$

where $J_{v'} = J_v + L$. Note, that the evaluation of vacuum expectation values $\langle \mathcal{O} | \dots | \mathcal{O} \rangle$ now implies a summation over all projections M_v , due to the degeneracy of the ground state. These excitations give rise to a single-particle contribution to the effective propagator:

$$\begin{aligned}
\tilde{D}_{00}^{\text{SP}}(\vec{r}, \vec{r}', E) &= \sum_{LM} B^{\text{SP}}(EL; J_v \rightarrow J_{v'}) \frac{2E_{J_{v'}}}{E^2 + E_{J_{v'}}^2 + i\eta} \\
&\quad \times F_L^{\text{SP}}(r) F_L^{\text{SP}}(r') Y_{LM}(\hat{r}) Y_{LM}^*(\hat{r}'). \quad (33)
\end{aligned}$$

Let us turn to collective core excitations. With the result

$$\begin{aligned}
&\sum_{M_\nu} \langle \mathcal{O} | \hat{Q}_{LM} | J_\nu M_\nu \rangle \langle J_\nu M_\nu | \hat{Q}_{L'M'}^\dagger | \mathcal{O} \rangle \\
&= \sum_m \langle \widetilde{\mathcal{O}} | \hat{Q}_{LM} | lm \rangle \langle lm | \hat{Q}_{L'M'}^\dagger | \widetilde{\mathcal{O}} \rangle \\
&= \delta_{lL'} \delta_{l'L} \delta_{MM'} B^{\text{core}}(EL; l \rightarrow 0), \quad (34)
\end{aligned}$$

one obtains (after relabeling summation indices)

$$\begin{aligned}
\tilde{D}_{00}^{\text{core}}(\vec{r}, \vec{r}', E) &= \sum_{LMJ_\nu} B^{\text{core}}(EL; L \rightarrow 0) \frac{2E_{J_\nu}}{E^2 - E_{J_\nu}^2 + i\eta} F_L^{\text{SP}}(r) F_L^{\text{SP}}(r') Y_{LM}(\hat{r}) Y_{LM}^*(\hat{r}') \\
&= \sum_{LM} \left(\sum_j \frac{2E_{L,j}}{E^2 - E_{L,j}^2 + i\eta} \right) B^{\text{core}}(EL; L \rightarrow 0) F_L^{\text{SP}}(r) F_L^{\text{SP}}(r') Y_{LM}(\hat{r}) Y_{LM}^*(\hat{r}'). \quad (35)
\end{aligned}$$

The summation over j runs over all members of the multiplet with $J_\nu = |J_\nu - L|, \dots, J_\nu + L$, which correspond to the core excitation of multipolarity L . According to Eq. (35) each state of the multiplet is associated with equal transition strength $B^{\text{core}}(EL)$. This may be not the case in reality. In view of the very small splittings between the excitation energies $E_{L,j}$, it may be legitimized to introduce an averaged eigenvalue \bar{E}_L labeling the collective core excitations. Thus, we can write

$$\begin{aligned}
\tilde{D}_{00}^{\text{core}}(\vec{r}, \vec{r}', E) &= \sum_{LM} B^{\text{core}}(EL; 0 \rightarrow L) \frac{2\bar{E}_L}{E^2 - \bar{E}_L^2 + i\eta} \\
&\quad \times F_L^{\text{SP}}(r) F_L^{\text{SP}}(r') Y_{LM}(\hat{r}) Y_{LM}^*(\hat{r}'). \quad (36)
\end{aligned}$$

In order to achieve a unique notation with respect to the expressions derived for collective vibrations, rotations, and giant resonances [7], we define as ‘‘collective’’ transition strengths: $B^{\text{coll}}(EL; L \rightarrow 0) := B^{\text{core}}(EL; 0 \rightarrow L) = (2L+1)B^{\text{core}}(EL; L \rightarrow 0)$. We can write the effective propagator for odd- A nuclei (suppressing the bars):

$$\begin{aligned}
\tilde{D}_{00}(\vec{r}, \vec{r}', E) &= \sum_{LM} \left\{ B^{\text{SP}}(EL; J_v \rightarrow J_{v'}) \frac{2E_{J_{v'}}}{E^2 - E_{J_{v'}}^2 + i\eta} \right. \\
&\quad \left. + B^{\text{coll}}(EL; L \rightarrow 0) \frac{2E_L}{E^2 - E_L^2 + i\eta} \right\} \\
&\quad \times F_L^{\text{SP}}(r) F_L^{\text{SP}}(r') Y_{LM}(\hat{r}) Y_{LM}^*(\hat{r}'). \quad (37)
\end{aligned}$$

TABLE I. The contributions $\Delta E_{\nu\kappa\mu}^{\tau}$ to the total energy shift due to various collective nuclear excitations τ are displayed for even- A thorium isotopes. Values for excitation energies and reduced transition probabilities are taken from Refs. [20–22]. For the giant dipole resonance (GDR) corresponding parameters are deduced according to the semiempirical formulas (A10) and (A11). Uncertain decimals are indicated in parentheses.

Isotope	Transition $\tau \equiv (k; L\pi; EL)$	Level E (MeV)	$B(EL; L \rightarrow 0)$ ($e^2 b^L$)	$ \Delta E_{1s_{1/2}}^{\tau} $ (meV)	$ \Delta E_{2s_{1/2}}^{\tau} $ (meV)	$ \Delta E_{2p_{1/2}}^{\tau} $ (meV)
$^{230}_{90}\text{Th}$	0; 2+; E2	0.0532	1.612	447.4	82.5	8.9
	0; 3-; E3	0.572	0.091	9.9	1.8	0.2
	2; 2+; E2	0.781	0.025	6.8	1.2	0.1
	1; 3-; E3	1.012	0.071	7.5	1.4	0.2
	GDR; E1	12.97	0.209	261.1	48.2	5.2
$^{232}_{90}\text{Th}$	0; 2+; E2	0.0495	1.842	505.2	93.2	10.1
	0; 2+; E2	0.7741	0.020	5.4	1.0	0.1
	0; 3-; E3	0.7744	0.064	6.9	1.3	0.1
	2; 2+; E2	0.785	0.024	6.4	1.2	0.1
	1; 3-; E3	1.106	0.037	4.0	0.7	0.(1)
	GDR; E1	12.94	0.211	262.8	48.5	5.3

Thus, the effective propagator decomposes into a collective and a single-particle contribution.

IV. NUMERICAL RESULTS

Let us now turn to the numerical results for the energy shifts of the $1s_{1/2}$, $2s_{1/2}$, and $2p_{1/2}$ states due to nuclear polarization in selected even- A actinide isotopes of Th, U, Pu, Cm, and Cf. Based on Eq. (14) the effective self-energy shifts for hydrogenlike ions are obtained after performing numerical integrations. We should mention, that only the contribution due to virtual transitions of the bound electron into the positive and negative energy continuum [first and third term of Eq. (14)] have

been taken into account. The contribution due to transitions in unoccupied bound states (second term) turns out to be negligible compared with the other terms. The evaluation proceeds according to the following scheme: For a given type of collective nuclear excitation (vibration, rotation, giant dipole resonance) the contribution of each single excitation of multipolarity L is calculated separately. For a fixed L , we first have to compute the radial matrix elements $\langle \nu\kappa | F_L | E'\kappa_1 \rangle$ between the considered electron bound state $|\nu\kappa\rangle$ and the intermediate continuum state $|E'\kappa_1\rangle$ with the radial function F_L of the corresponding effective propagator (see Appendix). In a second step the integration over the continuum energy E' is performed (see Ref. [7] for a more detailed discus-

TABLE II. The same as in Table I for even- A uranium isotopes. Values for excitation energies and reduced transition probabilities are taken from Refs. [20, 23–25]. Experimental uncertainties in the determination of the transition are indicated by “?”.

Isotope	Transition $\tau \equiv (k; L\pi; EL)$	Level E (MeV)	$B(EL; L \rightarrow 0)$ ($e^2 b^L$)	$ \Delta E_{1s_{1/2}}^{\tau} $ (meV)	$ \Delta E_{2s_{1/2}}^{\tau} $ (meV)	$ \Delta E_{2p_{1/2}}^{\tau} $ (meV)
$^{234}_{92}\text{U}$	0; 2+; E2	0.0435	2.180	707.5	132.9	15.3
	0; 3-; E3	0.850	0.084	10.6	2.0	0.2
	2; 2+; E2	0.927	0.025	7.8	1.5	0.2
	?; 3-; E3	1.023	0.031	3.9	0.7	0.(1)
	GDR; E1	12.91	0.214	313.2	58.8	6.8
$^{236}_{92}\text{U}$	0; 2+; E2	0.04524	2.320	747.1	140.3	16.2
	0; 3-; E3	0.745	0.076	9.4	1.8	0.2
	2; 2+; E2	0.959	0.036	11.2	2.1	0.2
	0; 3-; E3	1.040	0.044	5.4	1.0	0.1
	GDR; E1	12.89	0.216	314.8	59.1	6.8
$^{238}_{92}\text{U}$	0; 2+; E2	0.04491	2.460	786.4	147.7	17.0
	0; 3-; E3	0.732	0.082	10.1	1.9	0.2
	?; 3-; E3	0.998	0.029	3.4	0.6	0.(1)
	0; 2+; E2	1.037	0.013	4.0	0.8	0.(1)
	2; 2+; E2	1.060	0.026	8.0	1.5	0.2
	GDR; E1	12.86	0.217	316.5	59.5	6.9

TABLE III. The same as in Table I for even- A plutonium isotopes. Values for excitation energies and reduced transition probabilities are taken from Refs. [20, 26–29].

Isotope	Transition $\tau \equiv (k; L\pi; EL)$	Level E (MeV)	$B(EL; L \rightarrow 0)$ ($e^2 b^L$)	$ \Delta E_{1s_{1/2}}^T $ (meV)	$ \Delta E_{2s_{1/2}}^T $ (meV)	$ \Delta E_{2p_{1/2}}^T $ (meV)
$^{238}_{94}\text{Pu}$	0; 2+; E2	0.04408	2.526	961.2	184.0	22.6
	0; 3-; E3	0.661	0.101	14.8	2.8	0.4
	0; 2+; E2	0.983	0.024	8.8	1.7	0.2
	GDR; E1	12.86	0.219	375.3	71.8	8.9
$^{240}_{94}\text{Pu}$	0; 2+; E2	0.04282	2.666	1004.8	192.3	23.7
	0; 3-; E3	0.649	0.059	8.6	1.6	0.2
	2; 2+; E2	0.938	0.016	5.8	1.1	0.1
	GDR; E1	12.83	0.221	378.1	72.4	8.9
$^{242}_{94}\text{Pu}$	0; 2+; E2	0.0445	2.694	1009.8	193.3	24.1
	0; 3-; E3	0.833	0.060	8.6	1.6	0.2
	?; 3-; E3	1.020	0.064	9.1	1.7	0.2
	2; 2+; E2	1.102	0.031	11.2	2.1	0.3
	GDR; E1	12.80	0.222	380.2	72.8	9.0
$^{244}_{94}\text{Pu}$	0; 2+; E2	0.0460	2.722	1011.5	193.6	24.0
	?; 3-; E3	0.708	0.043	6.1	1.2	0.1
	or ?; 2+; E2		0.009	3.3	0.6	0.(1)
	?; 3-; E3	0.960	0.053	24.8	4.8	0.2
	or ?; 2+; E2		0.012	4.3	0.8	0.1
	?; 3-; E3	1.020	0.166	23.2	4.5	0.6
	or ?; 2+; E2		0.039	14.0	2.7	0.3
	?; 3-; E3	1.111	0.084	11.8	2.3	0.3
	or ?; 2+; E2		0.021	37.2	7.1	0.9
	GDR; E1	12.77	0.224	382.5	73.2	9.0

sion of the numerical procedure). We have tried to select isotopes, for which a considerable amount of experimental data for excitation energies and reduced transition strengths for collective vibrational and rotational states are available. The energy shifts presented due to the giant dipole resonance are results of pure model calculations, where the transition energies and the $B(EL)$ values are taken according to semiempirical formulas [Eqs. (A10), (A11)]. The results for the energy shifts due to

selected collective nuclear excitations will be tabulated in the following (see Tables I–V).

V. DISCUSSION OF THE RESULTS AND SUMMARY

A brief look at the tables presented in the previous section reveals, that the major contribution to the total energy shifts arises due to virtual excitation of the low-lying

TABLE IV. The same as in Table I for even- A curium isotopes. Values for excitation energies and reduced transition probabilities are taken from Ref. [30].

Isotope	Transition $\tau \equiv (k; L\pi; EL)$	Level E (MeV)	$B(EL; L \rightarrow 0)$ ($e^2 b^L$)	$ \Delta E_{1s_{1/2}}^T $ (meV)	$ \Delta E_{2s_{1/2}}^T $ (meV)	$ \Delta E_{2p_{1/2}}^T $ (meV)
$^{246}_{96}\text{Cm}$	0; 2+; E2	0.04285	2.988	1312.6	256.1	33.6
	2; 2+; E2	1.124	0.034	14.3	2.8	0.4
	1; 3-; E3	1.128	0.042	6.9	1.4	0.2
	0; 3-; E3	1.301	0.048	7.9	1.5	0.2
	3; 3-; E3	1.527	0.025	4.1	0.8	0.1
	1; 3-; E3	1.624	0.038	6.2	1.2	0.2
	GDR; E1	12.74	0.228	456.1	89.0	11.7
	$^{248}_{96}\text{Cm}$	0; 2+; E2	0.04338	2.998	1349.2	255.3
2; 2+; E2	1.050	0.036	15.1	2.9	0.4	
?; 3-; E3	1.100	0.059	9.7	1.9	0.2	
?; 3-; E3	1.235	0.021	3.4	0.7	0.(1)	
GDR; E1	12.71	0.229	458.8	89.5	11.8	

TABLE V. The same as in Table I for even- A californium isotopes. Values for excitation energies and reduced transition probabilities are taken from Ref. [30].

Isotope	Transition $\tau \equiv (k; L\pi; EL)$	Level E (MeV)	$B(EL; L \rightarrow 0)$ ($e^2 b^L$)	$ \Delta E_{1s_{1/2}}^{\tau} $ (meV)	$ \Delta E_{2s_{1/2}}^{\tau} $ (meV)	$ \Delta E_{2p_{1/2}}^{\tau} $ (meV)
$^{250}_{98}\text{Cf}$	0; 2+; E2	0.04272	3.200	1641.2	326.5	45.7
	2; 3-; E3	0.907	2.886	555.7	111.0	15.6
	1; 3-; E3	1.211	2.757	527.9	105.5	14.8
	?; 3-; E3	1.429	1.900	362.4	72.4	10.1
	GDR; E1	12.69	0.233	547.6	108.9	15.3
$^{252}_{98}\text{Cf}$	0; 2+; E2	0.04572	3.340	1636.5	325.6	45.6
	GDR; E1	12.66	0.234	550.5	109.5	15.4

rotational state and the giant dipole resonance. The main reason for that is obviously the relatively small excitation energy, respectively, the considerably large values for the reduced transition probabilities. All other modes taken into account contribute only at the percent level. The numerical values for the energy shifts of the $1s_{1/2}$, $2s_{1/2}$, and $2p_{1/2}$ states differ roughly by an order of magnitude, respectively. Summing up all the contributions referring to the excitations taken into account, we obtain values for the total energy shifts which are collected in Table VI. However, we should be aware about the uncertainties we have to deal with. Numerical errors are under control, since convergence of both the radial and the energy integration is achieved. The major source for deviations in the final numbers arises due to uncertainties in the values of the parameters [excitation energies and $B(EL)$ values] used in the calculation and due to the number of modes considered. The results for the contribution of the giant dipole resonance may be envisaged only as an estimate. Higher multipole resonances (e.g., the giant quadrupole resonance) should be included as well. In view of this

situation, we may assign a typical error of about 25% to the final energy corrections of the considered electron bound states. Nevertheless, it is instructive to plot all the results obtained for a given bound state, in order to get some insight into the general trend. In Fig. 3 the energy shifts of the $1s_{1/2}$ state is depicted. The actual contributions to the $2s_{1/2}$ - $2p_{1/2}$ Lamb shift is displayed in Fig. 4.

Let us briefly summarize. The theoretical approach of effective propagators has been extended to odd- A nuclei, which would allow us to take into account single-particle excitations of the valence proton. The derivation of the corresponding effective interaction was based on a microscopic approach utilizing the Weisskopf approximation. Accordingly, the resulting expression has a similar form as in the case of collective nuclear excitations.

We have presented numerical results for the energy correction of strongly bound electrons in hydrogenlike atoms due to nuclear polarization. Thereby, we have concentrated on a systematic study of the effect in even- A actinide isotopes. The contributions of nuclear polarization

TABLE VI. Total energy shifts (meV) of the $1s_{1/2}$, $2s_{1/2}$, and the $2p_{1/2}$ states and the contribution to the $2s_{1/2}$ - $2p_{1/2}$ Lamb shift due to the nuclear excitations collected in Tables I-V are shown.

Isotope	$ \Delta E_{1s_{1/2}} $ (meV)	$ \Delta E_{2s_{1/2}} $ (meV)	$ \Delta E_{2p_{1/2}} $ (meV)	$ \Delta E_{2s-2p} $ (meV)
$^{230}_{90}\text{Th}$	738.7	135.1	14.6	120.1
$^{232}_{90}\text{Th}$	790.7	145.9	15.8	130.1
$^{234}_{92}\text{U}$	1043.0	195.9	22.6	173.3
$^{236}_{92}\text{U}$	1087.9	204.3	23.5	180.8
$^{238}_{92}\text{U}$	1128.4	212.0	24.5	187.5
$^{238}_{94}\text{Pu}$	1360.1	260.3	32.1	228.2
$^{240}_{94}\text{Pu}$	1397.3	267.4	32.9	234.5
$^{242}_{94}\text{Pu}$	1418.9	271.5	33.8	237.7
$^{244}_{94}\text{Pu}$	1459.9	279.6	34.2	245.4
	or 1452.8	or 278.0	or 34.4	or 243.6
$^{246}_{96}\text{Cm}$	1808.1	352.8	46.4	306.4
$^{248}_{96}\text{Cm}$	1836.2	350.3	46.0	304.3
$^{250}_{98}\text{Cf}$	3634.8	824.3	201.5	622.8
$^{252}_{98}\text{Cf}$	2187.0	435.1	61.0	374.1

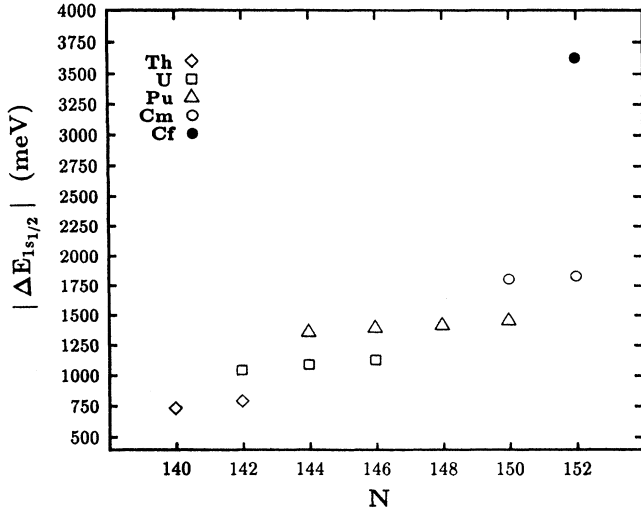


FIG. 3. Total energy shifts $|\Delta E_{1s_{1/2}}|$ in (meV) are shown for various isotopes as a function of the number of neutrons N .

to the actual $2s_{1/2}$ - $2p_{1/2}$ splitting turns out to be at least of the order of 0.1 eV and, thus, of the level of the current experimental accuracy.

ACKNOWLEDGMENTS

We would like to thank Ingvar Lindgren for interesting discussions during his visit at the Technische Universität Dresden. This work has been supported by the Bundesministerium für Forschung und Technologie (BMFT), by the Deutsche Forschungsgemeinschaft (DFG), by GSI (Darmstadt) and by NATO.

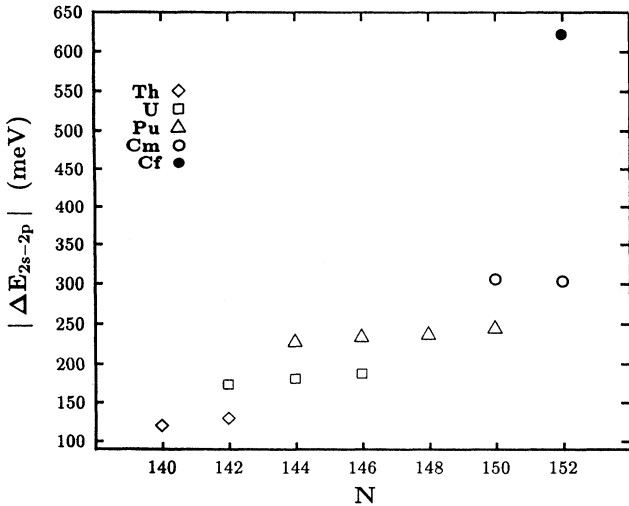


FIG. 4. Contributions $|\Delta E_{2s_{1/2}-2p_{1/2}}|$ in (meV) to the $2s_{1/2}$ - $2p_{1/2}$ Lamb shift are shown for various isotopes as a function of the number of neutrons N .

APPENDIX A: RADIAL FUNCTIONS AND REDUCED TRANSITION PROPABILITIES FOR COLLECTIVE NUCLEAR EXCITATIONS

1. Harmonic surface vibrator and free rotator

The collective dynamics of the nuclear surface can be treated in terms of collective bosons (surface phonons) [17]. Analytical expressions for the radial functions F_L and $B(EL)$ values can be derived. Let us note, that some intermediate formulas in the derivation of effective propagators appearing in Ref. [7] contain some obvious misprints. In the harmonic approximation, the following expression for the transition charge density (radial part) with multipolarity $L \geq 2$,

$$\mathcal{R}_L(r) = R_0^{-(L+2)} \delta(r - R_0), \quad (\text{A1})$$

can be derived. According to Eq. (10), one is led to radial functions,

$$F_L(r) = \frac{4\pi}{(2L+1)R_0^L} \left[\Theta(R_0 - r) \frac{r^L}{R_0^{L+1}} + \Theta(r - R_0) \frac{R_0^L}{r^{L+1}} \right]. \quad (\text{A2})$$

Specifying the set of excited nuclear states $|\nu\rangle$ as one-phonon states, i.e., $|\nu\rangle = |LM\rangle$, the Wigner-Eckart theorem applies when evaluating the matrix elements of the electric multipole transition operator \hat{Q}_{LM} . This leads to the reduced transition probabilities,

$$B^{\text{vib}}(EL; L \rightarrow 0) = (2L+1)^{-1} B^{\text{vib}}(EL; 0 \rightarrow L) = \frac{3}{4\pi} \frac{Z^2 L}{AmE_L} e^2 \hbar^2 R_0^{2(L-1)}, \quad (\text{A3})$$

where m denotes the mass of the nucleon.

Neglecting the effect of static nuclear quadrupole deformation the function $F_2(r)$ can be used to specify \tilde{D}_{00} in the case of low-lying rotational modes. The corresponding transition strengths $B(E2; 2K \rightarrow 0)$ depend on the quantum number K characterizing different rotational bands ($K = 0$ for the ground-state band, $K = 2$ for the γ band, etc).

2. Giant dipole resonance

Treating giant resonances within the hydrodynamical approach (HD) for spherical nuclei [17], one obtains transition charge densities (radial part),

$$\mathcal{R}_L^n(r) = \mathcal{N}_{Ln} j_L(z_{Ln} r) \Theta(R_0 - r), \quad (\text{A4})$$

with the normalization factor $\mathcal{N}_{Ln} = \left\{ \frac{1}{2} R_0^2 [j_L^2(z_{Ln}) - j_{L-1}(z_{Ln}) j_{L+1}(z_{Ln})] \right\}^{\frac{1}{2}}$. Accordingly, one derives the following radial functions [7]:

$$F_L^{(n)}(r) = \frac{4\pi}{(2L+1)R_0^L} \left\{ F_L(r) + \Theta(R_0 - r) \frac{2L+1}{R_0 z_{Ln}} \times \left[\frac{j_L(z_{Ln} r/R_0)}{j_{L+1}(z_{Ln})} - \left(\frac{r}{R_0} \right)^L \frac{j_L(z_{Ln})}{j_{L+1}(z_{Ln})} \right] \right\}, \quad (\text{A5})$$

where $z_{Ln} = k_{Ln}R_0$ are zeros determined by the boundary condition $(\frac{d}{dr}j_L(k_{Ln}r))|_{r=R_0} = 0$, and n labels the n th harmonic for a given multipolarity L . Corresponding transition strengths can be defined according to

$$\begin{aligned} B(EL; Ln \rightarrow 0) &= \frac{1}{2L+1} \sum_M |\langle \mathcal{O} | \hat{Q}_{LM}^{(n)} | LMn \rangle|^2 \\ &= \frac{3}{4\pi} \frac{ZNL}{AmE_{Ln}} \frac{2L}{z_{Ln}^2 - (L+1)} \\ &\quad \times e^2 \hbar^2 R_0^{2(L-1)}, \end{aligned} \quad (\text{A6})$$

where m denotes the mass of the nucleon. If one further assumes that the total strength of a giant resonance with multipolarity, L is concentrated at one energy $E_L \equiv E_{L1}$ referring to the lowest harmonic with $n = 1$, we can define a total $B(EL)$ value, e.g., for a giant dipole resonance ($L = 1$):

$$\begin{aligned} B(E1; 1 \rightarrow 0) &= \frac{1}{2} \sum_M |\langle \mathcal{O} | \hat{Q}_{LM} | 1M1 \rangle|^2 \\ &= \frac{3}{4\pi} \frac{ZN}{AmE_1} \frac{2}{z_{11}^2 - 2} e^2 \hbar^2. \end{aligned} \quad (\text{A7})$$

However, the physical quantity which is measured in the experiment is not a $B(E1)$ value but the photoabsorption cross section $\sigma(E)$ or the integrated cross section $\sigma = \int dE \sigma(E)$. Assuming that the dominant contribution to the total cross section is due to the giant dipole resonance only, we can write

$$\sigma^{\text{HD}}(E, \Gamma_1) = \frac{8\pi^2}{3\hbar c} B^{\text{HD}}(E1; 1 \rightarrow 0) \frac{E_1 \Gamma_1}{(E - E_1)^2 + \Gamma_1^2/4}. \quad (\text{A8})$$

Furthermore, neglecting the finite width Γ_1 of the giant

dipole resonance one finally obtains a total cross section,

$$\sigma_1^{\text{HD}} = \frac{16\pi^3}{3\hbar c} E_1 B^{\text{HD}}(E1; 1 \rightarrow 0) = \frac{8\pi^2}{z_{11}^2 - 2} \frac{ZN}{A} \frac{e^2 \hbar}{mc}. \quad (\text{A9})$$

The equation above allows us to deduce a transition strength for the giant dipole resonance from measurable quantities like the resonance energy and the photoabsorption cross section. It is known that the hydrodynamical model tends to overestimate such quantities. Instead of using (A9), it seems more appropriate to deduce the $B(E1)$ value from the semiempirical Thomas-Reiche-Kuhn (TRK) sum rule assuming again that it is completely fulfilled by the giant dipole resonance state:

$$\sigma_1^{\text{TRK}} = 2\pi^2 \frac{ZN}{A} \frac{e^2 \hbar}{mc} = \frac{16\pi^3}{3\hbar c} E_1 B^{\text{TRK}}(E1; 1 \rightarrow 0). \quad (\text{A10})$$

The excitation energy E_1 is determined according to the empirical formula [16, 14]:

$$E_1 = 95 \left(1 - A^{-1/3}\right) A^{-1/3} \text{ MeV}. \quad (\text{A11})$$

In the case of heavy nuclei the assumptions made above seem to be in good agreement with experimental data [19]. The $B(E1)$ values deduced from the hydrodynamical model and that obtained by the TRK sum rule are related by $B^{\text{HD}}(E1) \simeq 1.7 B^{\text{TRK}}(E1)$. Note, that the energy shifts calculated with transition strengths deduced from the TRK sum rule can be easily corrected by multiplication by an overall factor $q = (1 + \frac{\delta}{100})$. δ stands for the percentage to which the TRK sum rule may be exceeded or not. This parameter can be deduced from corresponding measurements of the photoabsorption cross section.

-
- [1] J. Schweppe, A. Belkacem, L. Blumenfeld, N. Claytor, B. Feinberg, H. Gould, V. E. Kostroum, L. Levy, S. Misawa, J. R. Mowat, and M. H. Prior, *Phys. Rev. Lett.* **66**, 1434 (1991).
- [2] S. A. Blundell, *Phys. Rev. A* **46**, 3762 (1992).
- [3] W. R. Johnson and G. Soff, *At. Data Nucl. Data Tables* **33**, 405 (1985).
- [4] G. Soff and P. J. Mohr, *Phys. Rev. A* **38**, 5066 (1988).
- [5] P. J. Mohr and G. Soff, *Phys. Rev. Lett.* **70**, 158 (1993).
- [6] G. Plunien, B. Müller, W. Greiner, and G. Soff, *Phys. Rev. A* **39**, 5428 (1989).
- [7] G. Plunien, B. Müller, W. Greiner, and G. Soff, *Phys. Rev. A* **43**, 5853 (1991).
- [8] P. Indelicato and E. Lindroth, *Phys. Rev. A* **46**, 2426 (1992).
- [9] K. T. Cheng, W. R. Johnson, and J. Sapirstein, *Phys. Rev. A* **47**, 1817 (1993).
- [10] H. Persson, I. Lindgren, S. Salomonson, and P. Sunnergren, *Phys. Rev. A* **48**, 2772 (1993).
- [11] H. Persson, I. Lindgren, and S. Salomonson, *Phys. Scr.* **T46**, 125 (1993).
- [12] I. Lindgren, H. Persson, S. Salomonson, V. Karasiev, L. Labzowsky, A. Mitrushenkov, and M. Tokman, *J. Phys. B* **26**, L503 (1993).
- [13] E. Borie and G. A. Rinker, *Rev. Mod. Phys.* **54**, 67 (1982).
- [14] B. Hoffmann, G. Baur, and J. Speth, *Z. Phys.* **315**, 57 (1984).
- [15] B. Hoffmann, G. Baur, and J. Speth, *Z. Phys.* **320**, 259 (1985).
- [16] P. Ring and P. Schuck, *The Nuclear Many Body Problem* (Springer, New York, 1980).
- [17] J. M. Eisenberg and W. Greiner, *Nuclear Models* (North-Holland, Amsterdam, 1987).
- [18] A. Bohr and B. R. Mottelson, *Struktur der Atomkerne*, Bd. 1 (Akademie-Verlag, Berlin, 1980).
- [19] B. L. Berman and S. C. Fultz, *Rev. Mod. Phys.* **47**, 713 (1975).
- [20] F. K. McGowan, C. E. Bemis, Jr., W. T. Milner, J. L. C. Ford, Jr., R. L. Robinson, and P. H. Stelson, *Phys. Rev. C* **10**, 1146 (1974).
- [21] Y. A. Ellis-Akovali, *Nucl. Data Sheets* **40**, 395 (1983).
- [22] M. R. Schmorak, *Nucl. Data Sheets* **63**, 145 (1991).
- [23] Y. A. Ellis-Akovali, *Nucl. Data Sheets* **40**, 540 (1983).

- [24] M. R. Schmorak, Nucl. Data Sheets **63**, 193 (1991).
[25] E. N. Shurshikov, Nucl. Data Sheets **53**, 612 (1988).
[26] E. N. Shurshikov, Nucl. Data Sheets **53**, 620 (1988).
[27] E. N. Shurshikov and N. V. Timoteeva, Nucl. Data Sheets **59**, 950 (1990).
[28] E. N. Shurshikov, M. L. Filchenkov, Y. F. Jaborov, and A. I. Khovanovich, Nucl. Data Sheets **45**, 515 (1985).
[29] E. N. Shurshikov, Nucl. Data Sheets **49**, 790 (1986).
[30] M. R. Schmorak, Nucl. Data Sheets **57**, 574 (1989).